

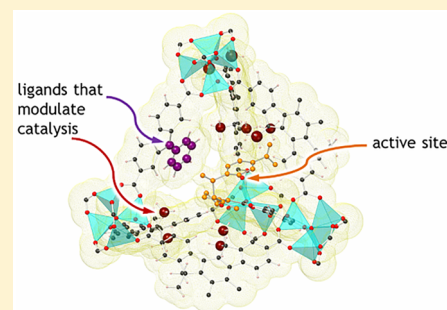
Modulating the Performance of an Asymmetric Organocatalyst by Tuning Its Spatial Environment in a Metal–Organic Framework

Lujia Liu,[†] Tian-You Zhou,[†] and Shane G. Telfer*[†]

MacDiarmid Institute for Advanced Materials and Nanotechnology, Institute of Fundamental Sciences, Massey University, Palmerston North 4442, New Zealand

S Supporting Information

ABSTRACT: Systematically tuning the spatial environment around the active sites of synthetic catalysts is a difficult challenge. Here, we show how this can be accomplished in the pores of multicomponent metal–organic frameworks. This relies on embedding a catalytic unit in a pore of the MUF-77 framework and then tuning its environment by introducing different functional groups to the surrounding linkers. This approach benefits from the structural regularity of MUF-77, which places each component in a precise location to circumvent disorder. Prolinyl groups, which are catalytically competent toward asymmetric aldol reactions, were selected as the catalytic unit. Since every prolinyl group is positioned in an identical environment, correlations between the pore architecture and the activity of these single-site catalysts can be elucidated. Systematic engineering of the pore structure, which is achieved by installing modulator groups on the framework linkers, impacts on the reaction rate and the enantiomeric excess of the aldol products. Furthermore, the spatial environment around the proline catalyst can override its innate stereochemical preference to dictate the preferred enantiomer of the reaction product. These results offer a new way to design three-dimensional active site environments for synthetic catalysts.



INTRODUCTION

The size, shape and chemical characteristics of the pores in metal–organic frameworks (MOFs) are central to their functional properties.¹ One established method of tuning the pore characteristics of MOFs is to introduce functional groups to the organic linkers. This is beautifully demonstrated by several isorecticular families of frameworks.^{2–4} The arrangement of two or more *different* functional groups in a MOF pore engenders more sophisticated chemical characteristics. One method to engineer such pores is to coassemble a set of linkers that share the same backbone into a multivariate MOF.⁵ Although such materials can exhibit interesting functional properties,^{6,7} the linkers are distributed in the lattice with a degree of randomness, which leads to pore heterogeneity.^{8–11} This will frequently be a disadvantage for applications such as catalysis and sensing, which benefit from architectural regularity. An alternative strategy of using two^{12–19} or three^{4,20–23} topologically distinct linkers to build up *multicomponent* MOFs²⁴ can preserve pore homogeneity. Since the linkers can be discriminated during framework assembly, they become positioned in unique lattice sites. We have shown that by installing functional groups on the organic linkers of the multicomponent MOFs MUF-7 and MUF-77, [Zn₄O-(bdc)_{1/2}(bpdc)_{1/2}(trig)_{4/3}] (bdc = 1,4-benzenedicarboxylate, bpdc = 4,4'-biphenyldicarboxylate, trig = 1,3,5-benzenetribenzoate or a truxene analogue) their pore architectures can be programmed.^{4,20} An important consequence of the lack of disorder in MUF-7 and MUF-77 is that structural regularity is

maintained upon functionalization. The pores in these frameworks feature a precise and predictable three-dimensional array of chemical groups. Given that these MOFs tolerate a diverse range of substituents on the linkers, they offer a unique platform to create pockets of chemical space with predefined characteristics that can be tuned with precision at the molecular scale.

Catalysts that are active and selective toward organic transformations are highly sought after. One method of enhancing the performance of abiological catalysts is to engage the reaction participants with specific noncovalent contacts with, for example, functional groups on the catalyst or the solvent.^{25–32} This relies on the sensitivity of the reaction outcome to perturbations to the energies of the competing transition states, which in turn is a function of the catalyst structure and its environment. An unmet challenge in this domain is the implementation of a well-defined array of noncovalent interactions in all three dimensions around a catalytic site. We propose that this can be achieved by exploiting the ability to engineer the chemical microenvironment of the multicomponent MUF-77 framework.

To implement this strategy, we first selected a catalytic unit to embed in MUF-77. Earlier work has established that effective heterogeneous catalysts can be generated by appending known organocatalytic units to the components of MOFs and related

Received: August 3, 2017

porous materials.^{33–38} We thus envisaged that a catalytic group could be installed on one of the three linkers of MUF-77 (Figure 1). If the linker that bears the catalytic unit has the

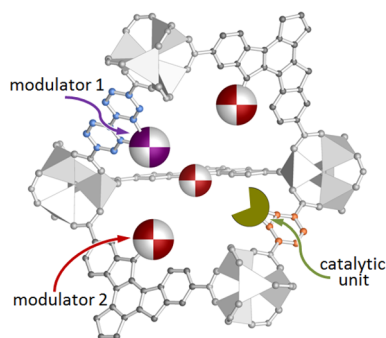


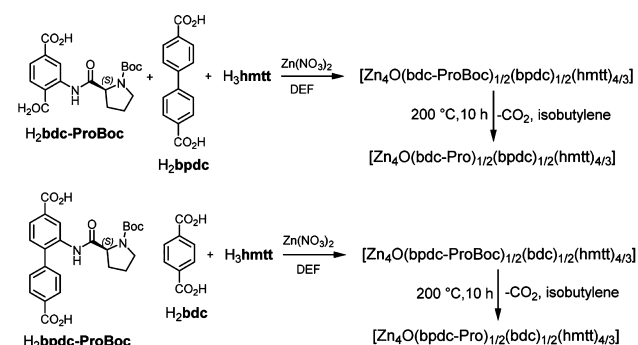
Figure 1. A schematic depiction of a pore in MUF-77 equipped with a site for catalysis and modulator groups that are positioned to influence the course of the reaction.

same backbone as one of the components of the MUF-77 framework it will specifically occupy the position of its parent linker in the lattice. A diverse range of organocatalytic moieties is amenable to this role, for example proline^{39,40} or urea,⁴¹ or groups that coordinate metal ions.^{42–44} Here, we opted for the prolinyl group since it has the advantages of being readily available in an enantiopure form, nontoxic, resistant to oxygen and water, and high activity under mild conditions (e.g., the addition of strong acids or bases is not required). The second aspect of our design strategy is the installation of *modulator* groups on the two linkers that do not bear the catalytic unit (Figure 1). We anticipated that, via noncovalent interactions with the reaction participants, these groups may be able to influence the reaction rate or alter the regioselectivity or stereoselectivity of product formation.

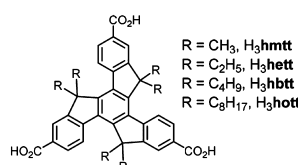
RESULTS AND DISCUSSION

Catalyst Synthesis and Structure. Our initial step was to introduce catalytically active prolinyl groups to MUF-77. Boc-protected (*S*)-prolinyl groups were appended to bdc and bpdc linkers by amide coupling reactions to give H₂bdc-ProBoc and H₂bpdc-ProBoc,³⁹ respectively (Figure 2a). The incorporation of bdc-ProBoc and bpdc-ProBoc into MUF-77 analogues was achieved using standard reaction conditions, viz the solvothermal reaction of three linkers (H₂bdc, H₂bpdc and 5,5',10,10',15,15'-hexamethyltruxene-2,7,12-tricarboxylic acid (H₃hmtt)) with Zn(NO₃)₂ in DEF. The structures of the resulting frameworks, [Zn₄O(bdc-ProBoc)_{1/2}(bpdc)_{1/2}(hmtt)_{4/3}] and [Zn₄O(bdc)_{1/2}(bpdc-ProBoc)_{1/2}(hmtt)_{4/3}], were determined by X-ray crystallography (SCXRD, Table S1). The lattice topology (itb-d) of both structures match the parent MUF-77 framework. Both the reflection and refinement statistics suggest that the framework model is best refined in the centrosymmetric *Pm*-3 space group despite the enantiopure (*S*)-prolinyl groups. This is due to the indistinct contributions made to the electron density maps by the chiral portion of the ligands. The existence of the intact ProBoc groups—along with the phase purity of the MOFs—was confirmed by ¹H NMR spectroscopy on dissolved samples. The integrals of the peaks of each of the three linkers perfectly matches those anticipated from the MOF stoichiometry (Figures S7, S15).

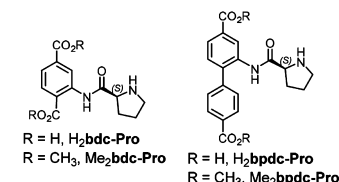
a Synthetic route to catalytically-active MUF-77 derivatives



b Tritopic truxene linkers



c Deprotected catalytic linkers



d Ditopic modulator linkers

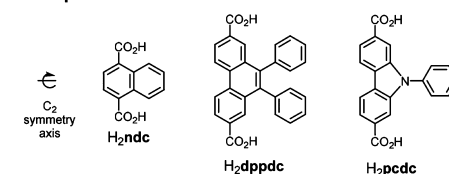
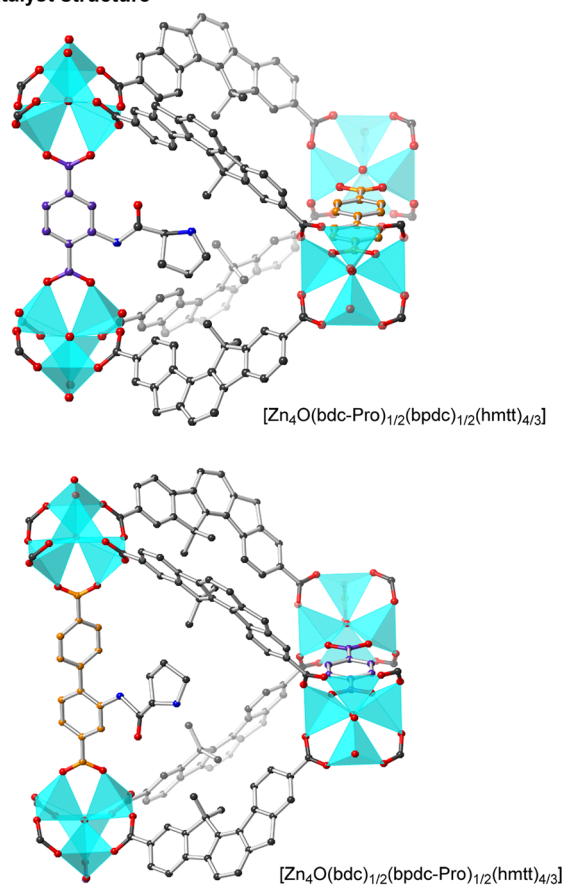


Figure 2. (a) The synthetic route to the Boc-protected MUF-77 derivatives and the thermolytic deprotection reaction that converts them into active catalysts. (b) The chemical structures of the tritopic truxene linkers used in this study. (c) The structures of R₂bdc-Pro and R₂bpdc-Pro. (d) The structures of the ditopic modulator ligands used in this study.

To deprotect the prolinyl units in [Zn₄O(bdc-ProBoc)_{1/2}(bpdc)_{1/2}(hmtt)_{4/3}] and [Zn₄O(bdc)_{1/2}(bpdc-ProBoc)_{1/2}(hmtt)_{4/3}] we simply heated the materials to 200 °C under vacuum to release the Boc groups as isobutylene and CO₂ using our previously established protocol (Figure 2a).^{45,46} The resulting MOFs are referred to as [Zn₄O(bdc-Pro)_{1/2}(bpdc)_{1/2}(hmtt)_{4/3}] and [Zn₄O(bdc)_{1/2}(bpdc-Pro)_{1/2}(hmtt)_{4/3}]. A combination of SCXRD (Table S1), powder X-ray diffraction (PXRD, Figures S25–S26), ¹H NMR spectroscopy (Figures S8, S14), and microscopy (Figures S58–S60) shows that the Boc groups are completely cleaved in this step and that the integrity of the lattice is maintained. We note that attempts to synthesize [Zn₄O(bdc-Pro)_{1/2}(bpdc)_{1/2}(hmtt)_{4/3}] and [Zn₄O(bdc)_{1/2}(bpdc-Pro)_{1/2}(hmtt)_{4/3}] directly from H₂bdc-Pro and H₂bpdc-Pro, respectively, led to undesired reactions of the prolinyl groups and limited catalytic activity (Figures S9, S15).

The structures of [Zn₄O(bdc-Pro)_{1/2}(bpdc)_{1/2}(hmtt)_{4/3}] and [Zn₄O(bdc)_{1/2}(bpdc-Pro)_{1/2}(hmtt)_{4/3}] were determined by single-crystal X-ray diffraction and are shown in Figure 3a. As previously observed for other members of the MUF-77 series, the three linkers are discriminated during framework assembly and each linker occupies a specific lattice site. Since the proline groups can occupy any one of four symmetry-related sites on the bdc or bpdc linkers it is remarkable that the first four atoms that extend away from the aryl ring could be found in the electron density difference map. The observation of these

a Catalyst structure



b Schematic of catalysis site

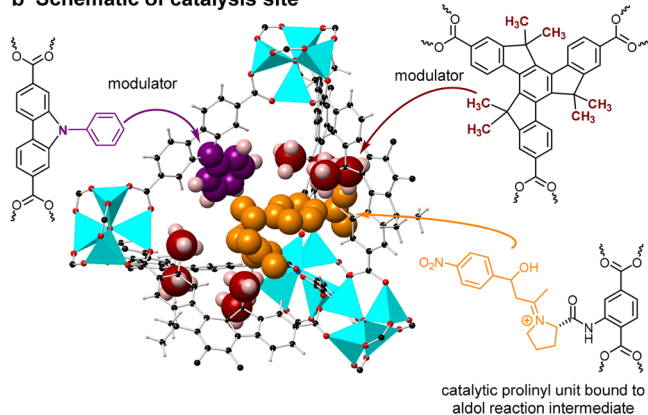


Figure 3. (a) The structures of $[\text{Zn}_4\text{O}(\text{bdc-Pro})_{1/2}(\text{bpdc})_{1/2}(\text{hmtt})_{4/3}]$ and $[\text{Zn}_4\text{O}(\text{bdc})_{1/2}(\text{bpdc-Pro})_{1/2}(\text{hmtt})_{4/3}]$ as deduced by X-ray crystallography. The prolinyl groups are shown in representative positions. Hydrogen atoms are omitted. (b) A schematic illustration of $[\text{Zn}_4\text{O}(\text{bdc-Pro})_{1/2}(\text{pcdc})_{1/2}(\text{hmtt})_{4/3}]$ bound to an aldol reaction intermediate to emphasize the potential contacts between the participants of the catalysis reaction and the modulator groups. The aldol intermediate is shown in orange, the methyl groups of hmtt in red, and the phenyl ring of the pcdc linker in violet.

atoms is made possible by the high crystallographic order of the lattice and the stability of the framework toward removal of occluded solvent molecules (that would otherwise produce background scatter). The atoms that could not be found crystallographically were placed in calculated positions. In Figure 3a the prolinyl groups are shown in representative positions

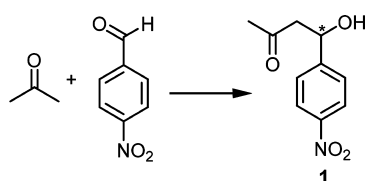
oriented toward the interior of a tetrahedral cavity defined by the bdc, bpdc and four hmtt linkers. All of the pores in these frameworks are crystallographically identical. An important corollary of this is that every prolinyl group is poised to operate in an equivalent environment in $[\text{Zn}_4\text{O}(\text{bdc-Pro})_{1/2}(\text{bpdc})_{1/2}(\text{hmtt})_{4/3}]$ and $[\text{Zn}_4\text{O}(\text{bdc})_{1/2}(\text{bpdc-Pro})_{1/2}(\text{hmtt})_{4/3}]$.

We subsequently designed modulator ligands to incorporate in the proline-containing frameworks. Our first consideration was that modulator linkers without suitable symmetry would not preserve the desired single-site nature of these catalysts. Second, the size of the functional groups appended to the modulator backbone is important. These groups must be large enough to exert an influence on the reaction occurring at the catalytic site but not so large that access by the reaction substrates is blocked. We used molecular modeling to assess this steric requirement. With these considerations in mind the ditopic modulators shown in Figure 2d were designed and synthesized. These linkers preserve a C_2 symmetry axis orthogonal to their long axes to maintain compatibility with the symmetry of the pore environment. To produce C_3 -symmetric tritopic modulators the methyl groups of hmtt were replaced by ethyl, butyl groups and octyl groups (hett, hbtt and hott, Figure 2b).

A model of a hypothetical catalytic site, which was produced by simple molecular modeling, is presented in Figure 3b. This schematic depicts an intermediate in the asymmetric aldol reaction of acetone and 4-nitrobenzaldehyde that is covalently bound to the prolinyl group in one of the pores of $[\text{Zn}_4\text{O}(\text{bdc-Pro})_{1/2}(\text{pcdc})_{1/2}(\text{hmtt})_{1/2}]$. This model emphasizes the potential for contacts between the van der Waals surfaces of the linkers and the reaction participants when reactions involving typical substrates take place at the proline site in this pore. The proximity of the phenyl ring of pcdc and the methyl groups of hmtt to the catalytic ensemble suggests that these—and similar—groups ought to be capable of imparting control over the catalyzed reaction via noncovalent interactions (that are either attractive or repulsive in nature). Although not shown, solvent molecules present in the pore are also likely to play a role. Here, we also make a brief comment about dynamic motion of the framework. On the basis of measurements on related MOFs,^{47,48} the bdc-Pro and bpdc-Pro linkers in MUF-77 are not expected to be static. Rather, they are likely to flip around their long axes on very short (\sim picosecond) time scales. A 180° flip of the catalytic linker will project the prolinyl group into a crystallographically identical pore. During this rotational motion the prolinyl group will sample the environment of the large dodecahedral pore of the MUF-77 framework. However, since all prolinyl groups in the framework will experience the same dynamic motion and time-averaged environment and their homogeneity will not be compromised.

The synthesis of MUF-77 type frameworks from sets of bdc/bpdc/truxene components (Figures 2b and 2d) was accomplished using conditions similar to those developed for the parent MOFs. In each case, a prolinyl group was installed on either the bdc linker (bdc-Pro) or the bpdc linker (bpdc-Pro). The ancillary ditopic ligand and the truxene linker served as modulator linkers. The combinations of linkers that were incorporated in the catalytic frameworks are summarized in Table 1. Powder X-ray diffraction (Figures S25–S26) together with ^1H NMR spectroscopy on dissolved samples (Figures S7–S23) demonstrate that the global structure of MUF-77 is preserved upon the introduction of these functionalized

Table 1. Aldol Reaction of Acetone and *p*-Nitrobenzaldehyde Catalyzed by MUF-77 Analogues with Installed bdc-Pro or bpdc-Pro Linkers^a



#	catalyst linker set	ee (%) ^b	k_{obs} ^c
1	bdc-Pro/bpdc/hmtt	-3.9 ± 0.6	0.74 ± 0.03
2	bdc/bpdc-Pro/hmtt	19.2 ± 1.1	0.52 ± 0.03
3	bdc-Pro/bpdc/hett	-3.9 ± 0.6	0.69 ± 0.04
4	bdc/bpdc-Pro/hett	17.0 ± 1.0	0.32 ± 0.02
5	bdc-Pro/bpdc/hbtt	4.2 ± 0.6	0.62 ± 0.02
6	bdc/bpdc-Pro/hbtt	18.3 ± 2.6	0.15 ± 0.01
7	bdc-Pro/bpdc/hott	1.8 ± 0.3	0.42 ± 0.02
8	bdc/bpdc-Pro/hott	15.7 ± 2.1	0.11 ± 0.01
9	ndc/bpdc-Pro/hmtt	24.2 ± 1.4	0.50 ± 0.02
10	ndc/bpdc-Pro/hbtt	18.1 ± 1.1	0.16 ± 0.01
11	ndc/bpdc-Pro/hott	19.1 ± 1.1	0.13 ± 0.01
12	bdc-Pro/pcdc/hmtt	-10.3 ± 1.4	0.052 ± 0.003
13	bdc-Pro/dppdc/hmtt	-26.5 ± 1.6	0.27 ± 0.01
14	bdc-ProBoc/bpdc/hmtt	n.r.	n.r.
15	bdc/bpdc-ProBoc/hmtt	n.r.	n.r.
<i>homogeneous catalysts</i>			
16	Me ₂ bdc-Pro	8.7 ± 1.2	3.94 ± 0.10
17	Me ₂ bpdc-Pro	30.3 ± 1.8	0.49 ± 0.01

^aStandard reaction conditions: 10 mol % catalyst (prolinyl units relative to total aldehyde), 0.04 M 4-nitrobenzaldehyde in acetone with 20 vol % H₂O at 20 °C. n.r. = no reaction. ^bEnantiomeric excess of product 1. A positive sign indicates the *R* enantiomer of the product is dominant and vice versa. ^cObserved rate constant based on the consumption of 4-nitrobenzaldehyde with units of L mol⁻¹ day⁻¹. Detailed data and information on standard deviation estimates are available in the SI.

components and that all samples are delivered in a phase-pure form. Any framework defects occur at exceedingly low levels, as can be inferred from (i) ¹H NMR spectroscopy on dissolved samples which showed the linkers to be present in the exact ratio defined by the framework stoichiometry, (ii) the absence of any visible impurities in these NMR spectra, (iii) the match between the simulated and experimental N₂ adsorption isotherms (Figures S32–S34) since it is well established that defective MOFs will lead to anomalous gas adsorption behavior,^{49–53} and (iv) the SCXRD refinement statistics and thermal displacement parameters, which are consistent with the full occupancy of all framework atoms.

These observations establish MUF-77 as a powerful and versatile platform for the development of a broad family of isorecticular heterogeneous catalysts in which the pore environment around the site of catalysis can be systematically tuned.

Catalysis Reactions. We found that the parent materials, [Zn₄O(bdc-Pro)_{1/2}(bpdc)_{1/2}(hmtt)_{4/3}] and [Zn₄O(bdc)_{1/2}(bpdc-Pro)_{1/2}(hmtt)_{4/3}], catalyze the asymmetric aldol transformation of 4-nitrobenzaldehyde and acetone to **1** (Table 1 Entries 1 and 2). This reaction was chosen as a model since it has been investigated in a range of other heterogeneous systems. We emphasize that our aim was not to produce an outstanding catalyst per se, but to use this reaction to develop the central concept of this report.

Preliminary screening experiments revealed that the reaction rate increases with added water, as observed for homogeneous catalysts,⁵⁴ and is independent of whether the reaction mixture is stood or tumbled. We settled on the following standard catalysis conditions: standing a heterogeneous mixture of the catalyst, acetone (≈1 mL, large excess), H₂O (20% v/v) and the aldehyde (0.04 M) at 20 °C. By running the reaction with increasing quantities of catalyst we established that the saturation loading of the catalyst, beyond which additional catalyst does not increase the reaction rate, is reached around a loading of ≈30 mol % of proline units (relative to the amount of aldehyde). At 10 mol % the reaction typically proceeded to completion over a period of ≈48 h. This became the standard catalyst quantity, which is in the typical range for organocatalysts. The reaction mixture was automatically sampled by HPLC every 120 min for 12 h and then again after 24 h (Figure S35). An observed rate constant, k_{obs} , was calculated based on the consumption of the aldehyde over the initial 12 h of the reaction (Figure 4a). The linearity of the pseudo-first-order kinetics plot over the entire course of the reaction was established by monitoring catalysis by [Zn₄O(bdc-Pro)_{1/2}(bpdc)_{1/2}(hmtt)_{4/3}] until complete consumption of the aldehyde (Figure S53). The ee was determined from HPLC chromatograms recorded after 24 h. A control reaction

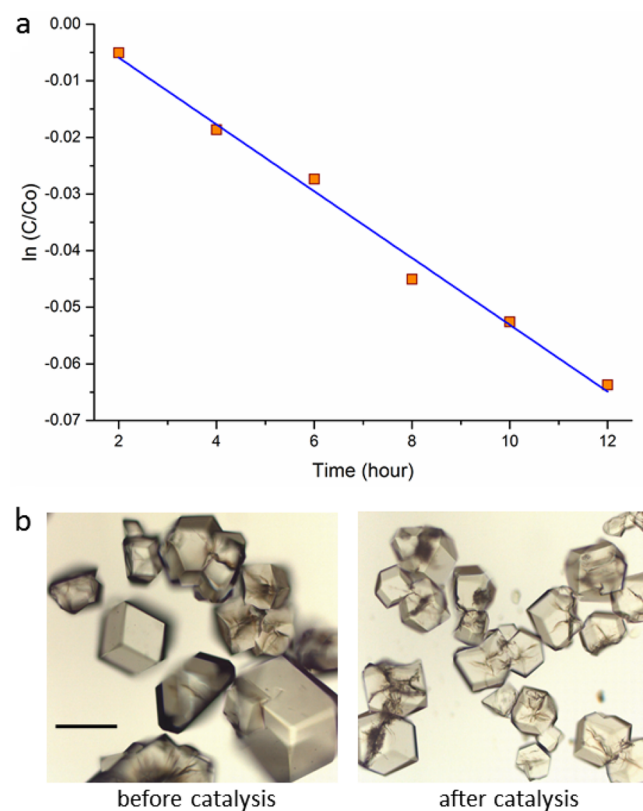


Figure 4. (a) A plot showing that the consumption of 4-nitrobenzaldehyde during its aldol reaction with acetone to produce **1** catalyzed by [Zn₄O(bdc)_{1/2}(bpdc-Pro)_{1/2}(hmtt)_{4/3}] exhibits pseudo-first-order kinetics. The orange squares are the measured data and the blue line is the least-squares minimized line of best fit to these points. C is the concentration of 4-nitrobenzaldehyde at time t , while C_0 is the initial concentration. (b) Optical micrographs of crystals of [Zn₄O(bdc)_{1/2}(bpdc-Pro)_{1/2}(hmtt)_{4/3}] before and after catalyzing the production of **1** demonstrate that their morphology and transparency is retained during catalysis (scale bar = 200 μm).

demonstrated that, as anticipated, frameworks with Boc-protected proline groups are catalytically inactive (Table 1, Entries 14 and 15). Further, to demonstrate the heterogeneous nature of the reaction, after several hours the catalysis mixture was filtered through a 0.45 μm filter to remove the MOF crystals. This halted the reaction, indicating that no catalytically active species are present in the supernatant.

Once this standard procedure had been established we developed a careful set of protocols to enable valid comparisons to be made between the various catalysts. We first verified that catalysts obtained from (i) independent synthetic batches, and (ii) different samples from the same batch led to reproducible k_{obs} and ee values (Tables S4–S5). This also allowed standard deviations of k_{obs} and ee to be estimated. We then examined the activity of the catalysts with modulator groups, and their k_{obs} and ee values are listed in Table 1. All of these catalysts produced linear pseudo-first-order kinetics plots (Figures S38–S48). As a further quality control measure, k_{obs} and the ee for the parent catalysts (Table 1, Entries 1 and 2) were redetermined several times during the period when data on the full set of catalysts was being acquired and were found to fall within one standard deviation of the listed values.

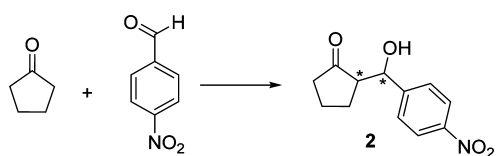
We found that $[\text{Zn}_4\text{O}(\text{bdc-Pro})_{1/2}(\text{bpdc})_{1/2}(\text{hmtt})_{4/3}]$ and $[\text{Zn}_4\text{O}(\text{bdc})_{1/2}(\text{bpdc-Pro})_{1/2}(\text{hmtt})_{4/3}]$ are recyclable catalysts. The crystals are unchanged after catalyzing the production of **1**, as indicated by PXRD (Figure S54), NMR spectroscopy (Figure S55), and optical microscopy (Figures 4b, S60). Following one reaction cycle, the crystals can be isolated by removal of the reaction supernatant, washed with fresh solvent and reused to catalyze a subsequent reaction. A series of five runs was conducted using the same catalyst (Figures S51–S52). The reaction rate remained constant over successive runs for $[\text{Zn}_4\text{O}(\text{bdc})_{1/2}(\text{bpdc-Pro})_{1/2}(\text{hmtt})_{4/3}]$, while a slight decrease was observed for $[\text{Zn}_4\text{O}(\text{bdc-Pro})_{1/2}(\text{bpdc})_{1/2}(\text{hmtt})_{4/3}]$. A similar drop in performance has been noted previously for some other heterogeneous catalysts with pyrrolidiny groups.^{35,36,39} In addition to demonstrating the recyclability of these catalysts, these results also illustrate their tolerance toward water, which comprises 20% of the reaction medium. This high degree of water stability was established for the parent MUF-77 framework in an earlier report.²⁰ It is somewhat uncommon for zinc(II)-carboxylate MOFs, and thus is an attractive characteristic of the MUF-77 catalyst family.

A series of telling conclusions may be drawn from the structural and catalysis data acquired in this study:

(1) The installation of prolinyl groups on the linkers to produce catalytically active analogues of MUF-77 does not perturb the structural characteristics of the parent framework and they remain well ordered. Therefore, these materials are genuine single-site^{55–60} catalysts and all the prolinyl groups in a given MOF exist in an identical microenvironment. This allows reliable structure–activity relationships to be established among this series of catalysts. Previously, important advances have been made by showing that the outcome of catalytic reactions in MOF pockets can be altered by modifying the pore structure.^{11,56,61} However, if each pore is not identical, for example due to incomplete postsynthetic modification reactions or framework disorder and defects, then the observed catalytic activity will stem from the ensemble of different pore environments.

- (2) The topography and chemistry of the catalytic pores in MUF-77 can be programmed by installing modulator linkers. Similar manipulations of catalytic pores have only been reported for a limited number of synthetic materials. For example, Long et al. observed that alkyl or fluoro groups installed adjacent to the catalytic metal sites of a series of Fe-MOF-74 analogues exerted a significant influence over the catalytic process,⁶² and Deria et al. reported the dependence of the product distribution of an acyl transfer reaction on lattice topology in a series of Zr-porphyrin MOFs.⁶³ MUF-77 analogues enable pore environments to be controlled with greater precision and diversity to build on these earlier breakthroughs.
- (3) The rate of the reaction catalyzed by bpdc-Pro is unaffected by its incorporation into the MUF-77 framework (Entry 2 vs 17). This demonstrates that heterogenization of a catalytic unit in a MOF does not necessarily introduce kinetic barriers such as hindered mass transport. The reaction rate of homogeneous Me₂bdc-Pro is higher than the MOFs containing the bdc-Pro linker (Entry 1 vs 16). We tentatively attribute this to an acceleration of the homogeneous reaction by beneficial noncovalent interactions between the carboxymethyl group and the reaction participants.
- (4) Modulator groups placed on linkers remote from the site of catalysis have a decisive impact on the asymmetric aldol reaction (Table 1). These results embody the successful realization of the central concept introduced by this study. When catalysis takes place at the bdc-Pro site and the tritopic linker is hmtt, replacing bpdc by the pcdc modulator results in a significant improvement in the ee of the aldol product **1** (Entries 1 vs 12). A further pronounced enhancement of the ee of **1** is induced by the dppdc modulator (Entry 13). Similar effects are apparent for catalysis taking place on the bpdc linker: the incorporation of ndc as a modulator boosts the ee of the reaction vis-à-vis bdc (Entry 9 vs Entry 2). Alkyl group modulators on the truxene ligand also have a discernible impact on the aldol reaction. The reaction occurring at bdc-Pro produces the *S* enantiomer of the product in excess when hmtt and hett are installed (Entries 1 and 3); however, the preference switches to the *R* enantiomer with hbtt and hott (Entries 5 and 7). When using bpdc-Pro as the catalytic linker, the ee is sensitive to the identity of the alkyl substituents on the truxene while the bdc linker is in place (Entries 2, 4, 6 and 8). This sensitivity is amplified when the bdc is replaced by ndc (Entries 9–11).
- (5) These results encouraged us to extend this study to the aldol reaction between cyclopentanone and *p*-nitrobenzaldehyde (Tables 2, S6). We selected four catalysts: the two parent catalysts together with those featuring modulator groups that had been found to exert considerable influence over the aldol reaction with acetone (dppdc and ndc). *Syn* and *anti* diastereoisomers are possible for **2** (Figure S56), and both of them exist as a pair of enantiomers. We found that $[\text{Zn}_4\text{O}(\text{bdc-Pro})_{1/2}(\text{bpdc})_{1/2}(\text{hmtt})_{4/3}]$ catalyzes the formation of **2** with a *syn:anti* ratio of 1.74:1, which changes to a ratio of 2.14:1 when bpdc is replaced by the dppdc modulator (Entries 1 and 3). Moreover, the ee of the *syn* diastereomer changes from –2.8% to 3.4%, and the ee

Table 2. Aldol Reaction of Cyclopentanone and *p*-Nitrobenzaldehyde Catalyzed by MUF-77 Analogues with Installed bdc-Pro or bpdc-Pro Linkers^a



#	catalyst linker set	dr ^b <i>syn:anti</i>	ee (%) ^c <i>syn anti</i>
1	bdc-Pro/bpdc/hmtt	1.74:1	-2.8 -35.8
2	bdc/bpdc-Pro/hmtt	0.55:1	37.2 16.8
3	bdc-Pro/dppdc/hmtt	2.14:1	3.4 -10.2
4	ndc/bpdc-Pro/hmtt	0.64:1	40.3 24.3

^aStandard reaction conditions: 10 mol % catalyst (prolinyl units relative to total aldehyde), 0.04 M 4-nitrobenzaldehyde in water-saturated cyclopentanone at 20 °C. The product distribution was determined by HPLC (Figure S57). ^bDiastereomeric ratio. ^cEnantiomeric excess of each of the two diastereomers of 2. Detailed information is available in the SI.

of the *anti* diastereomer is shifted from -35.8% to -10.2%. Similarly, when the catalyst is appended to the bpdc linker, the replacement of bdc by the ndc modulator has a noticeable impact on the product distribution (Entries 2 and 4).

The foregoing results demonstrate that a transformation catalyzed in a MOF pore can be influenced by a precise and tunable spatial array of modulator groups positioned remote from the site of catalysis. The modulator groups appear to act in synergy, rather than in a linear, additive fashion, and the properties of these catalysts is reminiscent of the emergent gas adsorption properties displayed by the MUF-7 series.⁴ We anticipate that the reaction mechanism parallels that generally accepted for related small-molecule catalysts.⁶⁴ While emphasis of the current study was not to optimize the catalyst performance per se, but to provide proof-of-concept, ongoing investigations are aimed at developing detailed insights into the key noncovalent interactions between the framework and the reaction participants. Elucidating these interactions with precision will be extremely challenging since (i) the prolinyl group undergoes dynamic motion, (ii) the magnitude of the variation in ee values indicates that the difference in diastereoisomeric transition states along the reaction pathway is very small, (iii) these energy differences will be influenced by a plethora of weak interactions of the catalytic intermediates with the modulator groups, and (iv) solvent effects may be important. Relevant investigations are underway in our laboratory. This knowledge will guide the rational design of modulator groups in next-generation catalysts that are able to exert an even more pronounced influence over the catalytic process to generate even higher reaction rates and enantioselectivities.

One unanticipated series of observations is that for the production of aldol product 1 [$Zn_4O(bdc-Pro)_{1/2}(bpdc)_{1/2}(trux)_{4/3}$] (*trux* = *hmtt*, *hett*) favor the *S* enantiomer while homogeneous $Me_2bdc-Pro$ favors the *R* enantiomer (Entries 1, 3, 16). Strikingly, this indicates that the spatial environment around the prolinyl group in these heterogeneous catalysts overrides its inherent enantioselectivity to control the stereochemical pathway of the reaction. The innate stereochemical preference⁴⁰ of the bdc-Pro catalyst can be restored by the installation of *hbtt* or *hott* modulator groups

(Entries 5 and 7). Further, if the prolinyl group is positioned on the bpdc linker the *R* enantiomer is preferentially generated by all catalysts. Similar observations were made for the aldol reaction that produces 2: the preferred enantiomer of both diastereomers can be reversed by switching the location of the catalytic group in the MOF.

Achieving stereochemical reversal in enantioselective transformations is a demanding challenge in asymmetric catalysis.^{65,66} It is valuable since both enantiomers of a reaction product can be obtained when only one hand of the catalyst is available, which is often the case for catalysts derived from natural products. To our knowledge, there are only two reported cases where the innate enantioselectivity of a catalyst is reversed by its inclusion in a MOF.^{67,68} There are surprisingly few examples of a reversal in enantioselectivity upon the heterogenization of a homogeneous catalyst in other materials.^{66,69} Our results go beyond these pioneering examples by establishing that the position of a catalytic site in a MOF can induce enantioselectivity reversal. Furthermore, the innate stereochemical preference of the catalyst can be restored by altering the catalysis microenvironment with wholly achiral modulators. These observations underscore the utility of being able to tune the catalysis microenvironment in multicomponent MOFs.

SUMMARY

This work establishes multicomponent frameworks as a powerful new class of heterogeneous catalysts in which modulator groups can be positioned in the pore to influence the catalytic transformation. Owing to the single-site nature of the catalytic pore, unambiguous correlations between framework modifications and the catalytic activity can be elucidated. The ability to design a three-dimensional microenvironment around the site of catalysis distinguishes multicomponent MOFs from conventional catalysts. Certain parallels exist between these MOFs and enzymes in that catalysis takes place at a specific site in a well-defined pocket and the reaction rate and stereochemical outcome are determined by interactions of the reaction components with a precisely positioned array of functional groups.^{70,71} Taking inspiration from protein engineering, where tuning the active site topology and chemistry is a well-established method for enhancing enzyme performance,⁷² systematic pore programming in multicomponent metal-organic frameworks offers opportunities to develop synthetic catalysts beyond the proof of principle examples presented here. For a given target reaction, we anticipate that a suitably engineered MOF catalyst can be optimized by, *inter alia*, modifying the catalytic unit, the nature and disposition of the modulator groups, and the lattice structure. These parameters define a vast combinatorial matrix that is capable of identifying high-performance catalysts.

ASSOCIATED CONTENT

Supporting Information

The Supporting Information is available free of charge on the ACS Publications website at DOI: 10.1021/jacs.7b07921.

Synthesis, characterization, X-ray crystallography details, kinetic analyses and additional tables and figures (PDF)
Crystal data (CIF)

AUTHOR INFORMATION

Corresponding Author

*s.telfer@massey.ac.nz

ORCID 

Lujia Liu: 0000-0001-9452-4371

Shane G. Telfer: 0000-0003-1596-6652

Author Contributions

†L.L. and T.-Y.Z. contributed equally.

Notes

The authors declare no competing financial interest.

ACKNOWLEDGMENTS

We are grateful to the RSNZ Marsden Fund for supporting this research (contract 14-MAU-024). We acknowledge the contribution of NeSI high-performance computing facilities and the MMIC to this research. We thank David Lun for his valuable technical assistance and Prof. Geoffrey Jameson, A/Prof. Guy Jameson and A/Prof. Gareth Rowlands for insightful discussions. L.L. is grateful for support from the China Scholarship Council for an outstanding Ph.D. student award and the RSNZ for the Hatherton Award.

REFERENCES

- (1) Furukawa, H.; Cordova, K. E.; O'Keeffe, M.; Yaghi, O. M. *Science* **2013**, *341*, 974.
- (2) Eddaoudi, M.; Kim, J.; Rosi, N.; Vodak, D.; Wachter, J.; O'Keeffe, M.; Yaghi, O. M. *Science* **2002**, *295*, 469–472.
- (3) Sim, J.; Yim, H.; Ko, N.; Choi, S. B.; Oh, Y.; Park, H. J.; Park, S.; Kim, J. *Dalton Trans.* **2014**, *43*, 18017–18024.
- (4) Liu, L.; Konstas, K.; Hill, M. R.; Telfer, S. G. *J. Am. Chem. Soc.* **2013**, *135*, 17731–17734.
- (5) Osborn Popp, T. M.; Yaghi, O. M. *Acc. Chem. Res.* **2017**, *50*, 532–534.
- (6) Xia, Q.; Li, Z.; Tan, C.; Liu, Y.; Gong, W.; Cui, Y. *J. Am. Chem. Soc.* **2017**, *139*, 8259–8266.
- (7) Deng, H.; Doonan, C. J.; Furukawa, H.; Ferreira, R. B.; Towne, J.; Knobler, C. B.; Wang, B.; Yaghi, O. M. *Science* **2010**, *327*, 846–850.
- (8) Park, T.-H.; Koh, K.; Wong-Foy, A. G.; Matzger, A. J. *Cryst. Growth Des.* **2011**, *11*, 2059–2063.
- (9) Burrows, A. D. *CrystEngComm* **2011**, *13*, 3623–3642.
- (10) Kong, X.; Deng, H.; Yan, F.; Kim, J.; Swisher, J. A.; Smit, B.; Yaghi, O. M.; Reimer, J. A. *Science* **2013**, *341*, 882–885.
- (11) Fracaroli, A. M.; Siman, P.; Nagib, D. A.; Suzuki, M.; Furukawa, H.; Toste, F. D.; Yaghi, O. M. *J. Am. Chem. Soc.* **2016**, *138*, 8352–8355.
- (12) Lin, Q.; Bu, X.; Kong, A.; Mao, C.; Zhao, X.; Bu, F.; Feng, P. *J. Am. Chem. Soc.* **2015**, *137*, 2235–2238.
- (13) Furukawa, H.; Ko, N.; Go, Y. B.; Aratani, N.; Choi, S. B.; Choi, E.; Yazaydin, A. O.; Snurr, R. Q.; O'Keeffe, M.; Kim, J.; Yaghi, O. M. *Science* **2010**, *329*, 424–428.
- (14) Helten, S.; Sahoo, B.; Bon, V.; Senkovska, I.; Kaskel, S.; Glorius, F. *CrystEngComm* **2015**, *17*, 307–312.
- (15) Grunker, R.; Bon, V.; Muller, P.; Stoeck, U.; Krause, S.; Mueller, U.; Senkovska, I.; Kaskel, S. *Chem. Commun.* **2014**, *50*, 3450–3452.
- (16) Klein, N.; Senkovska, I.; Gedrich, K.; Stoeck, U.; Henschel, A.; Mueller, U.; Kaskel, S. *Angew. Chem., Int. Ed.* **2009**, *48*, 9954–9957.
- (17) Yuan, S.; Lu, W.; Chen, Y. P.; Zhang, Q.; Liu, T. F.; Feng, D.; Wang, X.; Qin, J.; Zhou, H. C. *J. Am. Chem. Soc.* **2015**, *137*, 3177–3180.
- (18) Yuan, S.; Qin, J.-S.; Zou, L.; Chen, Y.-P.; Wang, X.; Zhang, Q.; Zhou, H.-C. *J. Am. Chem. Soc.* **2016**, *138*, 6636–6642.
- (19) Lee, S. J.; Doussot, C.; Telfer, S. G. *Cryst. Growth Des.* **2017**, *17*, 3185–3191.
- (20) Liu, L.; Telfer, S. G. *J. Am. Chem. Soc.* **2015**, *137*, 3901–3909.
- (21) Dutta, A.; Wong-Foy, A. G.; Matzger, A. J. *Chem. Sci.* **2014**, *5*, 3729–3734.
- (22) Lee, S. J.; Doussot, C.; Baux, A.; Liu, L.; Jameson, G. B.; Richardson, C.; Pak, J.; Trouselet, F.; Coudert, F.-X.; Telfer, S. G. *Chem. Mater.* **2016**, *28*, 368–375.
- (23) Qin, J.-S.; Du, D.-Y.; Li, M.; Lian, X.-Z.; Dong, L.-Z.; Bosch, M.; Su, Z.-M.; Zhang, Q.; Li, S.-L.; Lan, Y.-Q.; Yuan, S.; Zhou, H.-C. *J. Am. Chem. Soc.* **2016**, *138*, 5299–5307.
- (24) Qin, J.-S.; Yuan, S.; Wang, Q.; Alsalmeh, A.; Zhou, H.-C. *J. Mater. Chem. A* **2017**, *5*, 4280–4291.
- (25) Neel, A. J.; Hilton, M. J.; Sigman, M. S.; Toste, F. D. *Nature* **2017**, *543*, 637–646.
- (26) Toste, F. D.; Sigman, M. S.; Miller, S. J. *Acc. Chem. Res.* **2017**, *50*, 609–615.
- (27) Davis, H. J.; Phipps, R. J. *Chem. Sci.* **2017**, *8*, 864–877.
- (28) Giuliano, M. W.; Miller, S. J. *Top. Curr. Chem.* **2016**, *157*–201.
- (29) Raynal, M.; Ballester, P.; Vidal-Ferran, A.; van Leeuwen, P. W. N. M. *Chem. Soc. Rev.* **2014**, *43*, 1734–1787.
- (30) Raynal, M.; Ballester, P.; Vidal-Ferran, A.; van Leeuwen, P. W. N. M. *Chem. Soc. Rev.* **2014**, *43*, 1660–1733.
- (31) Meeuwissen, J.; Reek, J. N. H. *Nat. Chem.* **2010**, *2*, 615–621.
- (32) Miller, S. J. *Acc. Chem. Res.* **2004**, *37*, 601–610.
- (33) Yoon, M.; Srirambalaji, R.; Kim, K. *Chem. Rev.* **2012**, *112*, 1196–1231.
- (34) Chughtai, A. H.; Ahmad, N.; Younus, H. A.; Laypkov, A.; Verpoort, F. *Chem. Soc. Rev.* **2015**, *44*, 6804–6849.
- (35) Xu, H.; Gao, J.; Jiang, D. *Nat. Chem.* **2015**, *7*, 905–912.
- (36) Wang, C. A.; Zhang, Z. K.; Yue, T.; Sun, Y. L.; Wang, L.; Wang, W. D.; Zhang, Y.; Liu, C.; Wang, W. *Chem. - Eur. J.* **2012**, *18*, 6718–6723.
- (37) Rostamnia, S.; Doustkhah, E. *RSC Adv.* **2014**, *4*, 28238–28248.
- (38) Zhang, J.; Han, X.; Wu, X.; Liu, Y.; Cui, Y. *J. Am. Chem. Soc.* **2017**, *139*, 8277–8285.
- (39) Lun, D. J.; Waterhouse, G. I. N.; Telfer, S. G. *J. Am. Chem. Soc.* **2011**, *133*, 5806–5809.
- (40) Bonnefoy, J.; Legrand, A.; Quadrelli, E. A.; Canivet, J.; Farrusseng, D. *J. Am. Chem. Soc.* **2015**, *137*, 9409–9416.
- (41) Roberts, J. M.; Fini, B. M.; Sarjeant, A. A.; Farha, O. K.; Hupp, J. T.; Scheidt, K. A. *J. Am. Chem. Soc.* **2012**, *134*, 3334–3337.
- (42) Jeong, K. S.; Go, Y. B.; Shin, S. M.; Lee, S. J.; Kim, J.; Yaghi, O. M.; Jeong, N. *Chem. Sci.* **2011**, *2*, 877.
- (43) Cho, S.-H.; Ma, B.; Nguyen, S. T.; Hupp, J. T.; Albrecht-Schmitt, T. E. *Chem. Commun.* **2006**, 2563–2565.
- (44) Thacker, N. C.; Lin, Z.; Zhang, T.; Gilhula, J. C.; Abney, C. W.; Lin, W. *J. Am. Chem. Soc.* **2016**, *138*, 3501–3509.
- (45) Deshpande, R. K.; Minnaar, J. L.; Telfer, S. G. *Angew. Chem., Int. Ed.* **2010**, *47*, 4598–4602.
- (46) Gupta, A. S.; Deshpande, R. K.; Liu, L.; Waterhouse, G. I. N.; Telfer, S. G. *CrystEngComm* **2012**, *14*, 5701–5704.
- (47) Gould, S. L.; Tranchemontagne, D.; Yaghi, O. M.; Garcia-Garibay, M. A. *J. Am. Chem. Soc.* **2008**, *130*, 3246–3247.
- (48) Jiang, X.; Duan, H.-B.; Khan, S. I.; Garcia-Garibay, M. A. *ACS Cent. Sci.* **2016**, *2*, 608–613.
- (49) Shearer, G. C.; Chavan, S.; Bordiga, S.; Svelle, S.; Olsbye, U.; Lillerud, K. P. *Chem. Mater.* **2016**, *28*, 3749–3761.
- (50) Ghosh, P.; Colon, Y. J.; Snurr, R. Q. *Chem. Commun.* **2014**, *50*, 11329–11331.
- (51) Liang, W.; Coghlan, C. J.; Ragon, F.; Rubio-Martinez, M.; D'Alessandro, D. M.; Babarao, R. *Dalton Trans.* **2016**, *45*, 4496–4500.
- (52) Thornton, A. W.; Babarao, R.; Jain, A.; Trouselet, F.; Coudert, F. X. *Dalton Trans.* **2016**, *45*, 4352–4359.
- (53) Bueken, B.; Reinsch, H.; Reimer, N.; Stassen, I.; Vermoortele, F.; Ameloot, R.; Stock, N.; Kirschhock, C. E. A.; De Vos, D. *Chem. Commun.* **2014**, *50*, 10055–10058.
- (54) Zotova, N.; Franzke, A.; Armstrong, A.; Blackmond, D. G. *J. Am. Chem. Soc.* **2007**, *129*, 15100–15101.
- (55) Pelletier, J. D. A.; Basset, J.-M. *Acc. Chem. Res.* **2016**, *49*, 664–677.

- (56) Cohen, S. M.; Zhang, Z.; Boissonnault, J. A. *Inorg. Chem.* **2016**, *55*, 7281–7290.
- (57) Metzger, E. D.; Brozek, C. K.; Comito, R. J.; Dincă, M. *ACS Cent. Sci.* **2016**, *2*, 148–153.
- (58) Li, Z.; Schweitzer, N. M.; League, A. B.; Bernales, V.; Peters, A. W.; Getsoian, A. B.; Wang, T. C.; Miller, J. T.; Vjunov, A.; Fulton, J. L.; Lercher, J. A.; Cramer, C. J.; Gagliardi, L.; Hupp, J. T.; Farha, O. K. *J. Am. Chem. Soc.* **2016**, *138*, 1977–1982.
- (59) Manna, K.; Ji, P.; Lin, Z.; Greene, F. X.; Urban, A.; Thacker, N. C.; Lin, W. *Nat. Commun.* **2016**, *7*, 12610.
- (60) Rogge, S. M. J.; Bavykina, A.; Hajek, J.; Garcia, H.; Olivos-Suarez, A. L.; Sepulveda-Escribano, A.; Vimont, A.; Clet, G.; Bazin, P.; Kapteijn, F.; Daturi, M.; Ramos-Fernandez, E. V.; Llabres i Xamena, F. X.; Van Speybroeck, V.; Gascon, J. *Chem. Soc. Rev.* **2017**, *46*, 3134–3184.
- (61) Yuan, S.; Chen, Y.-P.; Qin, J.-S.; Lu, W.; Zou, L.; Zhang, Q.; Wang, X.; Sun, X.; Zhou, H.-C. *J. Am. Chem. Soc.* **2016**, *138*, 8912–8919.
- (62) Xiao, D. J.; Oktawiec, J.; Milner, P. J.; Long, J. R. *J. Am. Chem. Soc.* **2016**, *138*, 14371–14379.
- (63) Deria, P.; Gómez-Gualdrón, D. A.; Hod, I.; Snurr, R. Q.; Hupp, J. T.; Farha, O. K. *J. Am. Chem. Soc.* **2016**, *138*, 14449–14457.
- (64) Cheong, P. H.-Y.; Legault, C. Y.; Um, J. M.; Çelebi-Ölçüm, N.; Houk, K. N. *Chem. Rev.* **2011**, *111*, 5042–5137.
- (65) Bartók, M. *Chem. Rev.* **2010**, *110*, 1663–1705.
- (66) Escorihuela, J.; Burguete, M. I.; Luis, S. V. *Chem. Soc. Rev.* **2013**, *42*, 5595–5617.
- (67) Zheng, M.; Liu, Y.; Wang, C.; Liu, S.; Lin, W. *Chem. Sci.* **2012**, *3*, 2623.
- (68) Niefing, S.; Czekelius, C.; Janiak, C. *Catal. Commun.* **2017**, *95*, 12–15.
- (69) García, R. A.; Van Grieken, R.; Iglesias, J.; Sherrington, D. C.; Gibson, C. L. *Chirality* **2010**, *22*, 675–683.
- (70) Lillerud, K. P.; Olsbye, U.; Tilset, M. *Top. Catal.* **2010**, *53*, 859–868.
- (71) Nath, I.; Chakraborty, J.; Verpoort, F. *Chem. Soc. Rev.* **2016**, *45*, 4127–4170.
- (72) Toscano, M. D.; Woycechowsky, K. J.; Hilvert, D. *Angew. Chem., Int. Ed.* **2007**, *46*, 3212–3236.